

Appendix

Table of Contents

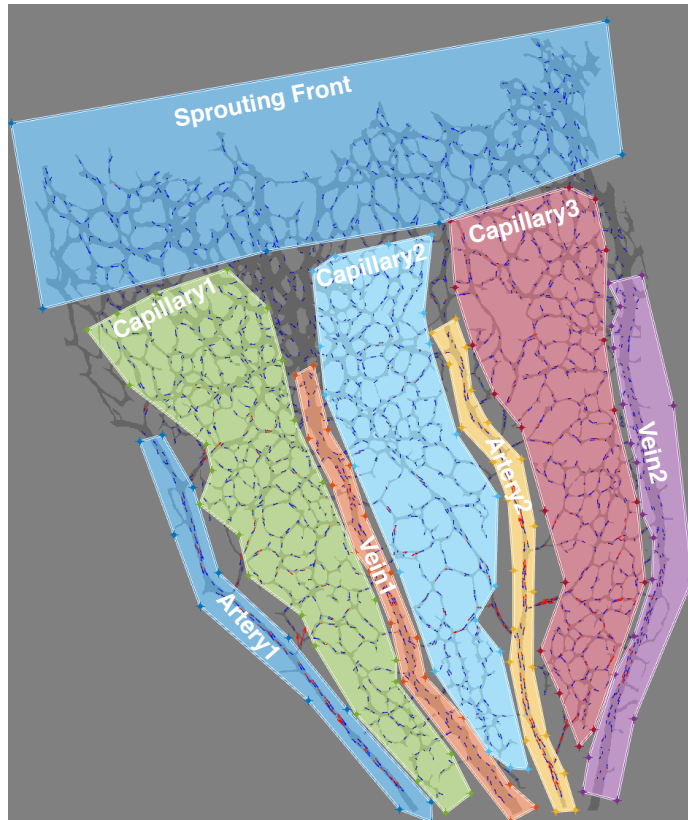
Appendix Figures

- P1 Figure S1. Flow-dependent polarity patterns of endothelial cells in control and *Pard3^{iAEC}*.
- P2 Figure S2. The effect of PAR-3 on VCAM-1 in isolated ECs from mouse aorta.
- P3 Figure S3. Further confirmation of the effect of loss of PAR-3 on endothelial cellular response.
- P4 Figure S4. Rho-Kinase regulates balance between the PAR-3/aPKC λ complex versus the aPKC λ /GSK3 β complex
- P5 Figure S5. GSK3 β indirectly controls EC polarity toward the flow axis and anti-inflammatory effects *in vitro*

Appendix legends

P6-8

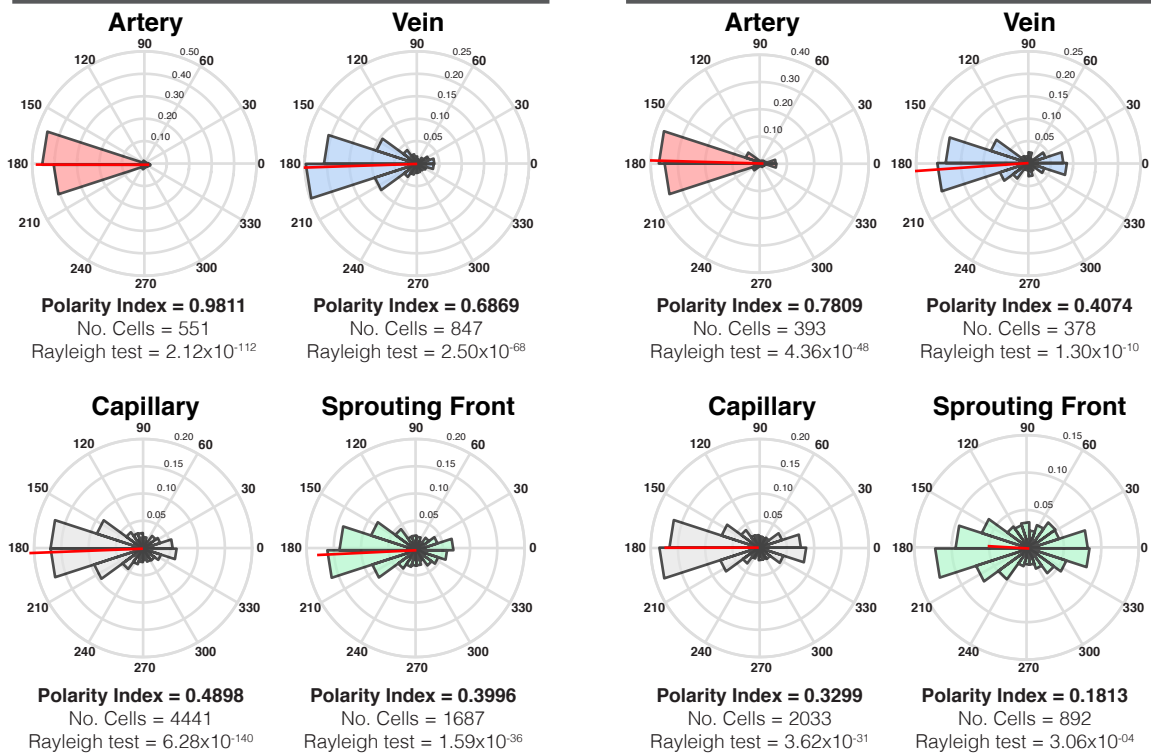
A *Pard3* WT (segmentation example)



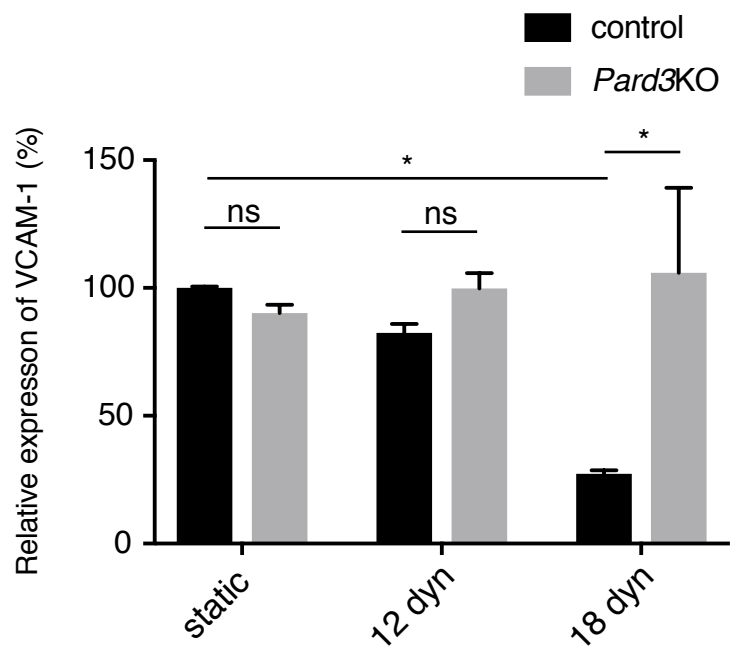
B

Pard3 WT

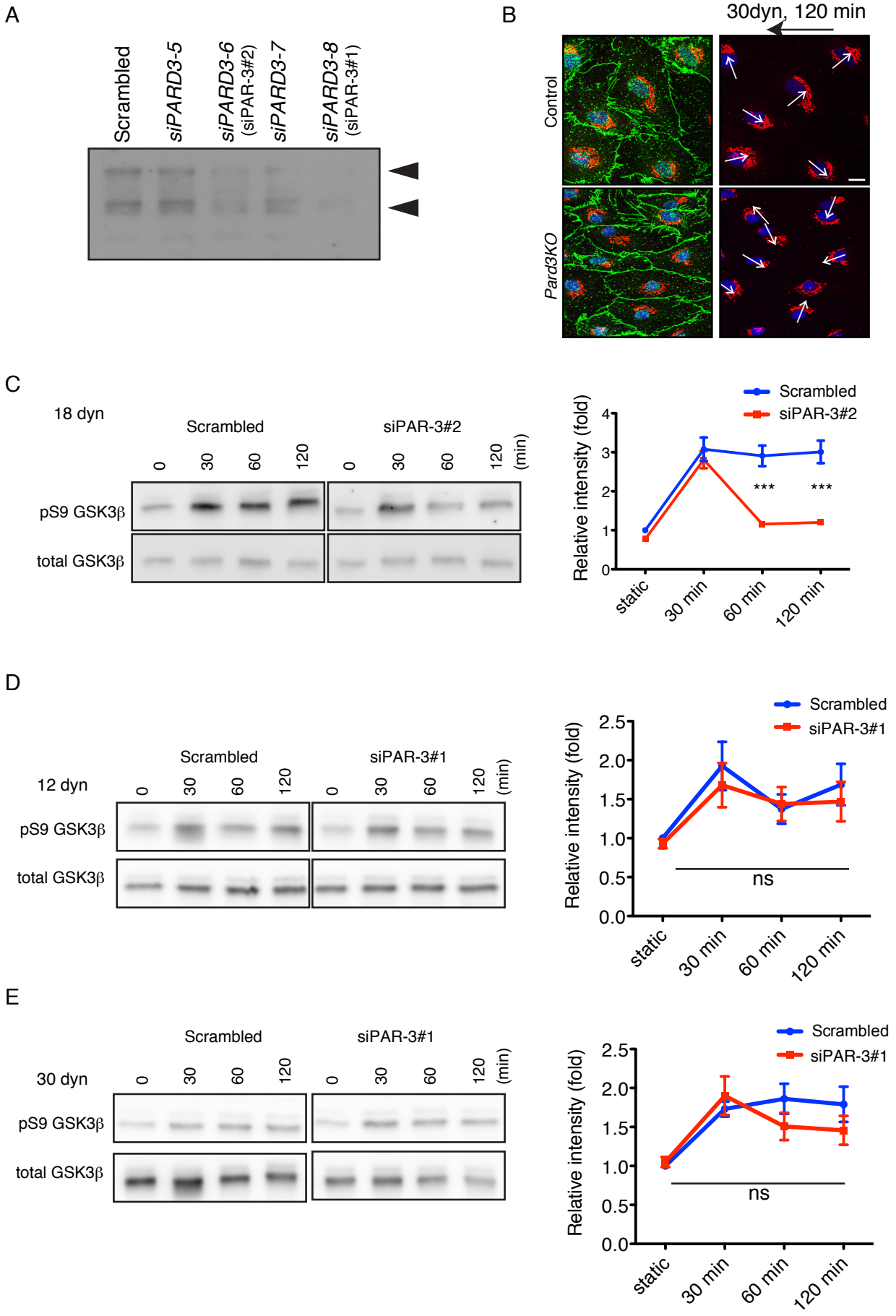
Pard3 Δ EC



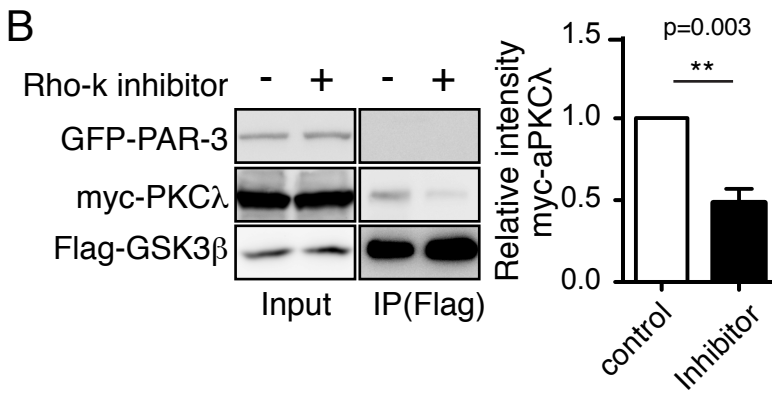
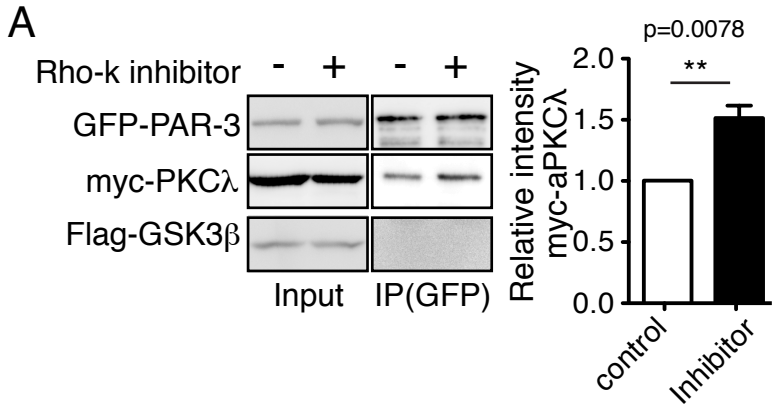
Appendix Figure S1



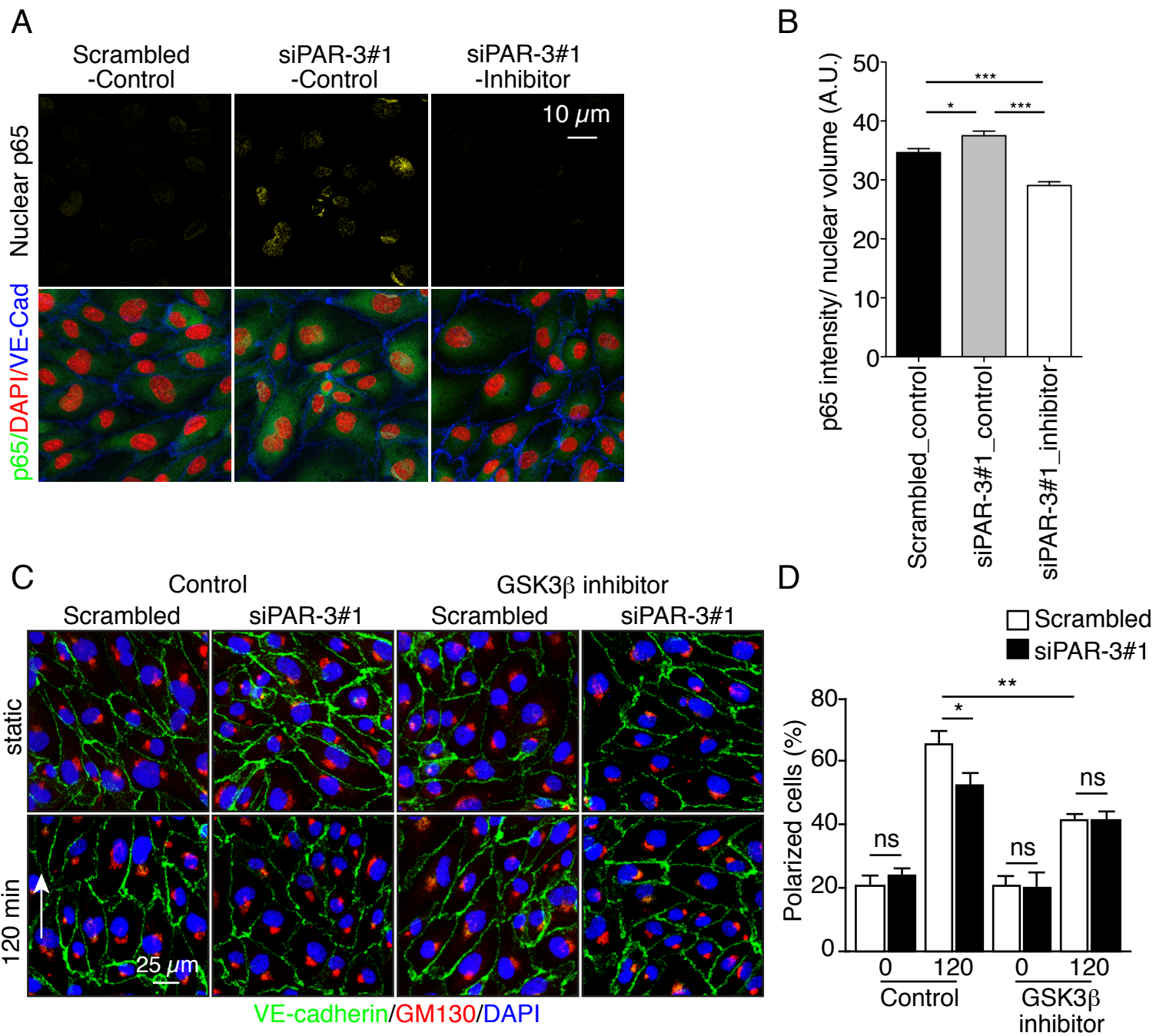
Appendix Figure S2



Appendix Figure S3



Appendix Figure S4



Appendix Figure S5

Appendix legends

Appendix Figure S1. Flow-dependent polarity patterns of endothelial cells in control and *Pard3*^{iΔEC}.

A. Overview of segmentation strategy for each specific vascular bed in a *Pard3* WT P6 mouse retina. The network is segmented in 4 types of vascular beds: arteries, veins, capillary network and vascular sprouting front. The specific image contains 2 arteries, 2 veins, 3 capillary networks and 1 sprouting front. All endothelial cells in each specific vascular bed is then pooled together to obtain a global polarity pattern for each specific mouse retina.

B. Angular histograms of endothelial cell polarity patterns for the designated vascular beds, as described in (A) for control and *Pard3*^{iΔEC} P6 mouse retinas. Polarity indexes are calculated as described in the material and methods and Figure 1B; total number of cells for each angular histogram; statistical Rayleigh test for non-uniform distribution of cell polarities. n=3 animals.

Appendix Figure S2. The effect of PAR-3 on VCAM-1 in isolated ECs from mouse aorta.

Effect of laminar flow on VCAM-1 expression level of the control and KO aortic ECs. In B, data are mean ± SEM (n=3 experiments); statistical significance (*p < 0.05) was evaluated with tow-way ANOVA followed by Tukey's post-test for multiple comparisons. ns: not significant, P≥0.05; differences: **P<0.01.

Appendix Figure S3. Further confirmation of the effect of loss of PAR-3 on endothelial cellular response.

A. WB of *siPAR3*s transfected ECs. Most efficient one (#8; siPAR-3#1) and second best (#6; siPAR-3#2) were used in this study. B Endothelial cells isolated from P56 *Pard3^{fllox/fllox}; Cdh5-CreERT2* mouse aorta were seeded in the fibronectin-coated flow chamber and gene knockout was induced by incubating cells with 1 μ M 4-Hydroxytamoxifen. PBS was used as control. After 48 hours, ECs were exposed to 30dyn/cm² laminar flow for 120 min, and axial polarity was analyzed. EC junction (VE-cadherin) is green, Golgi (GM130) is red, and nuclear stain (DAPI) is blue. White arrows show the direction of the vector from the center of EC nuclei to Golgi. C. Confirmation of PAR-3 KD phenotype using another siRNA. HUVECs transfected with siPAR-3#2 were treated with 18dyn/cm² of laminar flow and subjected to western blotting with indicated antibodies. Quantitation is shown on the right side. D, E, Effect of low flow (12dyn/cm²) and high flow (30dyn/cm²) on GSK3 β S9 phosphorylation. HUVECs were transfected with siPAR-3#1 and subjected to 12dyn/cm² (upper panels) or 30dyn/cm² (lower panels) of laminar flow. Quantitation is shown on the right side of images. In C, D and E, data are means \pm SEM (n=3 experiments); ns: not significant, P \geq 0.05; differences: ***P<0.001, analyzed with 2-way ANOVA followed with Bonferroni multiple comparisons. Scale bar, 10 μ m.

Appendix Figure S4. Rho-Kinase regulates balance between the PAR-3/aPKC λ complex versus the aPKC λ /GSK3 β complex

A, B. HEK293 cells were transfected with indicated cDNAs and were treated with or without Rho-kinase inhibitor (Y-27632, 20 μ M). After immunoprecipitation with indicated antibodies, samples were analyzed by Western blotting. In A and B data are presented as mean \pm SEM (n=5 experiments). Differences **P<0.01 were analyzed with Mann–Whitney U test.

Appendix Figure S5. GSK3 β indirectly controls EC polarity toward the flow axis and anti-inflammatory effects *in vitro*

A, Representative images of control and PAR-3KD ECs treated with control or GSK3 β inhibitor (6-BIO, 1 μ M) under static condition or after subjected to 18dyn/cm² flow for 120 min. The direction of flow is indicated on the picture. EC junction (VE-cadherin) is green, Golgi (GM130) is red, and nuclear stain (DAPI) is blue. B, Quantitative analysis of the percentile of ECs polarized at 90° degrees toward the flow direction. C, Nuclear translocation of p65 on the control (scrambled) and PAR-3 KD ECs, subjected to 12 dyn/cm² flow for 60 min, with culture medium containing control (DMSO) or GSK3 β inhibitor (1 μ M 6-BIO). D, Quantification and statistical analysis/ In B and D, data are means \pm SEM of three independent experiments, n=100 cells from each experiment; ns: not significant, P \geq 0.05; differences: statistical significance (*p < 0.05; **p<0.01; ***p<0.001) was evaluated with one-way ANOVA with Tukey's multiple comparison post hoc analysis. Scale bars, 10 μ m (A) and 25 μ m (C).